



Measurement of Seawater Flow-Induced Erosion Rates for Iron Surfaces using Thin Layer Activation Technique

Imam Kambali* & Hari Suryanto

Center for Radioisotope and Radiopharmaceutical Technology (PTRR),
National Nuclear Energy Agency (BATAN)
Puspiptek Area, Serpong, SouthTangerang, Indonesia

*E-mail: imamkey@batan.go.id

Abstract. The laboratory-scale erosion-corrosion testing facility at BATAN's Center for Radioisotope and Radiopharmaceutical Technology (PTRR) in Serpong was employed to simulate flow-induced corrosion of iron surfaces. Surface loss rates were measured by a nuclear technique called thin layer activation (TLA) analysis. A 10-MeV proton beam generated from a typical CS-30 cyclotron was used to produce ^{56}Co radionuclide layers on iron surfaces via a $^{56}\text{Fe}(p,n)^{56}\text{Co}$ nuclear reaction. The labeled iron specimens were then exposed to circulating seawater simulated in BATAN's flow-induced corrosion test facility. The experimental results indicated that the TLA technique was able to measure a very low flow-induced erosion rate of $0.91 \pm 0.3 \mu\text{m/hr}$. There was no significant difference in the measured surface loss rates between the remaining activity method and the concentration method. The iron surface loss in seawater was lower than that of the same material in HCl solution observed in earlier studies.

Keywords: ^{56}Co radionuclide; cyclotron; flow-induced corrosion; nuclear technique; thin layer activation (TLA).

1 Introduction

Thin layer activation (TLA) is a nuclear technique previously developed to help measure very low wear and erosion-corrosion rates of industrial components [1-6]. It involves target irradiation using a beam of charged particles such as protons, deuterons, He-3 and He-4 or neutrons to directly label the surface of interest (widely called a coupon) with a very thin layer containing radioactive isotopes (a few hundred μm thick). Following the target irradiation, the activated surface layer is exposed to a flowing corrosive fluid. This is eventually followed by measurement of its radioactivity ratio before and after erosion-corrosion takes place. The radioactivity loss is directly proportional to the surface loss and therefore its erosion-corrosion rate can be determined precisely [7]. In order to get information on the surface loss of the coupon specimen, a calibration curve, which represents the relationship between radioactivity ratio and surface loss, must first be prepared by means of either a stacked-foil or an abrasion method [8]. Also, theoretical calibration curves can

Received January 6th, 2016, 1st Revision August 18th, 2016, 2nd Revision September 13th, 2016, Accepted for publication September 26th, 2016.

Copyright ©2016 Published by ITB Journal Publisher, ISSN: 2337-5779, DOI: 10.5614/j.eng.technol.sci.2016.48.4.9

be calculated for a given projectile, beam current, energy, target geometry and irradiation time [8].

Two methods have been developed to measure the radioactivity loss of a specimen/coupon, i.e. the remaining activity method and the concentration method. The remaining activity method measures the radioactivity left over in the coupon at a certain time during the erosion-corrosion process and then compares the radioactivity with a calibration curve prepared earlier to obtain the corresponding surface loss. On the other hand, the concentration method detects the specific radioactivity removed from the coupon's surface, after which the same procedures as in the first method are applied.

Flow-induced corrosion (sometimes also called erosion-corrosion) of iron-based materials occurs frequently to industrial components, which can lead to great problems partly due to their relatively difficult position to conduct measurements. Moreover, conventional methods such as gravimetry, ultrasound methods, etc. cannot be used properly to measure very slow degradation processes [8]; thus a nuclear technique such as TLA analysis is expected to help overcome these issues.

Singh and co-workers [9] bombarded several targets, such as $^{63,65}\text{Cu}$, ^{59}Co , ^{93}Nb and $^{121,123}\text{Sb}$, to create thin radioactive layers of $^{66,67,68}\text{Ga}$, ^{61}Cu , $^{96\text{g,m}}\text{Tc}$ and $^{123,124,126}\text{I}$, respectively, using up to 400 nA α -particles. They suggest that the radioactive layers can be employed to study the wear rates of materials containing Cu, Co, Nb and Sb. Meanwhile, using 8-MeV deuteron beams, Craciun, *et al.* [10] measured the wear rates of Cr-plated and phosphated piston rings and discovered that the Cr-plated piston rings wore off at a rate nearly 5 times higher than the phosphated piston rings. Similar measurements on piston rings and cylinder housings have recently been reported by Chowdury, *et al.* [11], whereas flow-induced corrosion of carbon steel was determined by Subramanian and co-workers [12] using a thin ^{56}Co layer produced by proton beam irradiation via a $^{56}\text{Fe}(\text{p},\text{n})^{56}\text{Co}$ nuclear reaction. These recent investigations confirmed the use of the TLA technique for wear and erosion-corrosion measurements.

Corrosion of steel plate in seawater has been theoretically modeled by Soares, *et al.* [13], who highlighted the dependence of the corrosion rates on seawater temperature and velocity. While there has been an overwhelming number of iron-based corrosion measurements using conventional methods, to the best of the authors' knowledge no work has been published on measuring the degradation rate of iron in seawater using the TLA method; thus it is useful to test this nuclear technique for such purpose.

This paper discusses the use of the nuclear/TLA technique to measure flow-induced corrosion rates of iron surfaces in seawater. Two methods—the remaining activity method and the concentration method—were employed and compared to each other in detecting radioactivity during the experiments.

2 Experiments and Calculations

2.1 Target Preparation and Irradiation

The target of interest was prepared in the form of a pure iron coupon (99.995% purity) with a diameter of 1 cm and a thickness of 1 cm, which was then mounted on a target holder. Even though the standard carbon steel coupon thickness is 3.2 mm, a 1-cm thick coupon was chosen in this investigation for an easy and doable experimental setup, particularly the attachment of the coupon to the holder (a 3.2 mm thick coupon would have been difficult to attach to the available holder). The coupon thickness is less important and will not influence the experimental results when it is thicker than the total expected surface loss during the experiment.

The target was placed in such a way that the proton beam with a 1-cm diameter was aligned properly and would hit the target perpendicularly as the beam was directed to the target (note that the target could be tilted as required). An aluminum degrader was employed to reduce the proton energy in front of the aluminum collimator, as illustrated in Figure 1. The thickness of the Al degrader could be adjusted so that the required proton energy was met. In this experiment, a 2.85-mm Al foil was required to reduce the proton energy from 26.5 MeV to 10 MeV. The iron target was irradiated at a dose of 1.2 $\mu\text{A}\cdot\text{hr}$.

Based on the TALYS calculated $^{56}\text{Fe}(p,n)^{56}\text{Co}$ nuclear cross-section [14] and some earlier experimental data [8,10], the optimum cross-sections lie in the proton energy range between 8 and 13 MeV; thus 10 MeV was set as the incident energy of the incoming protons. Lower energy than 10 MeV may result in lower radioactivity, which eventually leads to difficulties in measuring, whereas a much higher energy will result in enhanced safety concerns. No radioactivity is expected to occur should the proton beam irradiate the iron specimen at an energy level lower than 5.4 MeV.

Following the target irradiation, a thin layer containing radioactive isotopes (in the order of micrometers) was formed on the target surface. After a 20-hour cooling time, the radioactivity of the coupon targets was analyzed on the basis of their spectrum by measuring the gamma rays emitted from the radioactive isotopes using a portable gamma ray spectroscopy system consisting of a 76×76 mm-NaI(Tl) detector, which was connected to a multi channel analyzer

(MCA) covering an energy range between 0 MeV and 1.8 MeV (1024 channel numbers) with an energy resolution of nearly 50 keV around the peak of a Cs-137 source ($E_\gamma = 0.662$ MeV). The portable MCA (Type MCA8000A, serial number 2278) was made by Amptek, USA. The spectroscopy system was calibrated using multiple gamma rays from Co-60 ($E_\gamma = 1.17$ MeV and 1.33 MeV), Cs-137 ($E_\gamma = 0.662$ MeV) and Ir-192 ($E_\gamma = 0.308$ MeV; 0.317 MeV; 0.468 MeV; 0.604 MeV and 0.612 MeV) radioactive sources. The NaI(Tl) detector's efficiency was better than 90% at a photon energy of 0.5 MeV and 80% at a photon energy of 1 MeV, whereas the count rate was in the range of 0 to 200,000 counts per second.

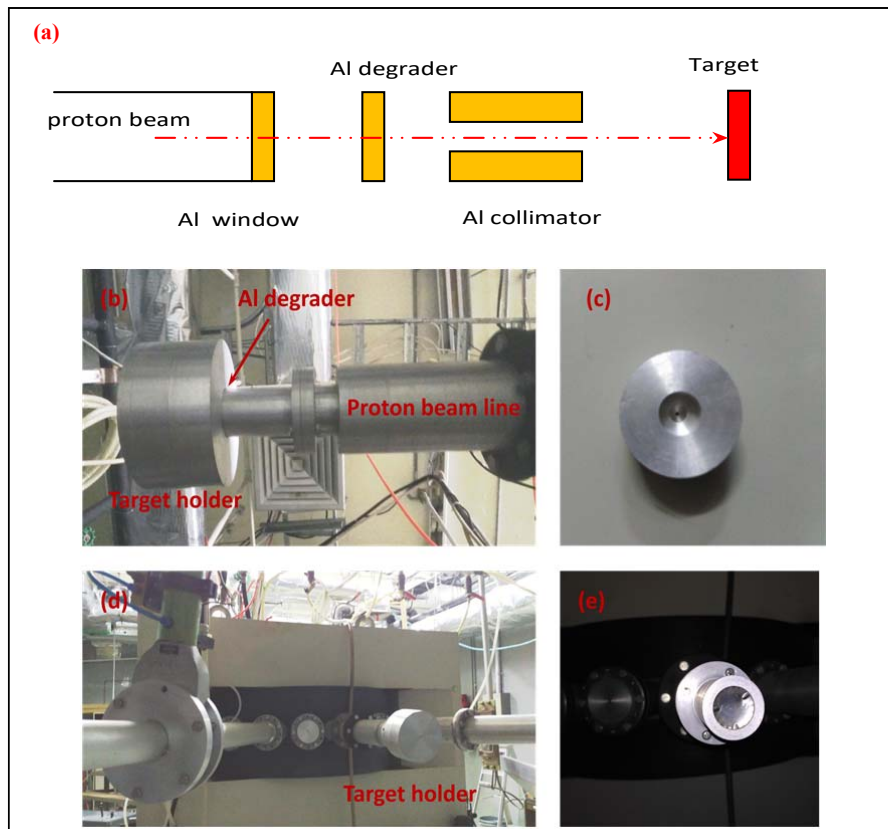


Figure 1 (a) Sketch of a typical experimental setup for target irradiation as described elsewhere [11]. (b) Top view of the experimental setup. (c) Target holder. (d) Front view of the experimental setup. (e) Aluminum degrader.

While the energy resolution of an HPGe detector is better than that of an NaI(Tl) detector, the latter has better sensitivity compared to the HPGe detector, which means that the NaI(Tl) detector captures more gamma rays than the HPGe detector. For this experiment, a detector with better sensitivity, i.e. an NaI(Tl) detector), was preferred since the measured activity was relatively low.

2.2 Calibration Curves

One of the most important characteristics of a radioactive layer is the depth distribution of the radionuclides on the target surface, which is represented by the calibration curve used for converting the radioactivity ratio to the surface loss. In this experiment the calibration curve was prepared by the stacked-foil method as described by Kambali, *et al.* in [15], which is very similar to the target preparation and irradiation procedures except for the target of interest, which was replaced by a stack of 30 iron foils (purchased from Goodfellow, Inc., UK), 10 μm thick and 2 cm in diameter, respectively. The uncertainty of the 10- μm thick foils was 15% each. The stacked foils were irradiated with a 10-MeV proton beam at a dose of 0.5 μAhr . The radioactivity of the proton-induced radionuclide in the stacked foils was eventually measured using the gamma ray spectroscopic system after a 20-hour cooling time.

2.3 Flow-Induced Erosion Equipment and Surface Loss Measurement

The surface degradation of the iron specimens/coupons was simulated at laboratory scale, in which the samples were exposed to a flow-induced corrosion (FIC) fluid. Two different fluids were simulated and compared in this experiment, namely seawater (with salinity at 3.2% and pH at 7.8) as well as a solution of seawater and 0.001 M HCl. PTRR-BATAN previously designed and constructed an FIC testing facility (shown in Figures 2(a) and 2(b)), which is capable of simulating a wide range of degradation experiments. The FIC facility consists of a 0.5-m high tank (900 liters in volume), where the flowing fluid is stored and circulated in a polyvinyl chloride (PVC) pipe with a diameter of 10 cm by pumping up the fluid into the pipe at a fixed volumetric flow of 100 liter/minute and a constant pressure of 20 bar. The TLA coupon was mounted in a prepared hole in the pipe so that the coupon surface was parallel to the pipe wall and then exposed to the flowing fluid. The Amptek portable gamma ray spectrometer, consisting of an NaI(Tl) detector which stayed in a holder under the pipe, was employed to measure the radioactivity of the coupon every 2 hours as the fluid was flowing. The rate of flow-induced corrosion was determined from the radioactivity ratio for a certain time by the assistance of the calibration curve. The total measuring time was 18 hours. Two methods—the remaining activity method and the concentration method, as described in the

Introduction section—were compared in this experiment. Note that the temperature of the flowing seawater was kept at room temperature (25°C) during the experiments.

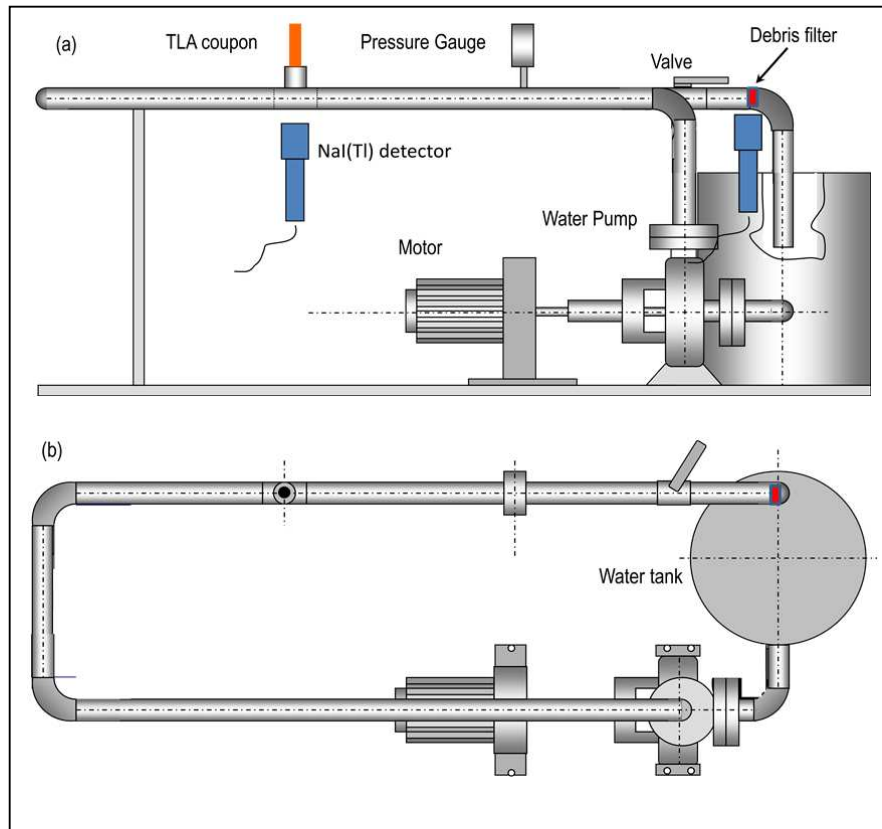


Figure 2 Schematic drawings of the FIC testing facility at PTRR-BATAN viewed from behind (a) and top (b).

In the concentration method measurement, an oil/debris filter was installed near the tank to ensure that there was no significant ^{56}Co debris flowing back into the system; instead it was trapped in the filter, thus preventing it to be re-measured in the flow. The NaI(Tl) detector was placed in front of the debris filter near the tank (as can be seen in Figure 2(b)) to measure the radioactivity of ^{56}Co debris. Radioactivity measurement indicated that no significant ^{56}Co debris was detected in the flow after the flowing liquid had passed through the oil filter. It was also found that the radioactivity loss of the TLA coupon was comparable to that recorded in the filter. Note that the concentration method measurement was

conducted in a separate experiment with the same experimental parameters as used for the remaining activity method.

Theoretical calculations were also performed using the stopping and range of ion in matter (SRIM) codes [16] to estimate the range of the 10-MeV proton beams in the iron target. In the calculations, using the SRIM-2013 version, nearly 100,000 protons were simulated to hit the 99.995% pure iron target at an incident angle of 0° relative to the incoming proton beam. Note that the SRIM codes have been widely used and proven to be in a good agreement with experimental results at accuracy of more than 10% [17].

3 Results and Discussion

3.1 Calculated Range of Protons in Iron Targets

Based on the SRIM-2013 code calculations, a 10-MeV proton beam is able to penetrate through an iron target at an average range of 257.4 μm . This calculated result is essential, particularly to determine the appropriate thickness of the iron target so that the proton beam stops in the target. The prepared iron targets (1 cm thick) as well as the stacked iron foils (300 μm thick) in the experiments were therefore thick enough to completely stop the proton beam. According to the latest TALYS calculated nuclear cross-sections (version 1.8) [14], the threshold energy for a $^{56}\text{Fe}(p,n)^{56}\text{Co}$ nuclear reaction is 5.4453 MeV. Therefore, for 10-MeV proton beam incidence in an Fe target, the expected depth of the radioactive layer is 166.3 μm , whereas the non-radioactive layer is 93.71 μm (between a depth of 166.3 μm and 260.01 μm).

3.2 Spectrum of ^{56}Co Radionuclide

Based on nuclear cross-section data reported earlier [18-19], a 10-MeV proton beam is able to cause nuclear transmutation of ^{56}Fe to become ^{56}Co via a $^{56}\text{Fe}(p,n)^{56}\text{Co}$ nuclear reaction. The ^{56}Co radionuclide decays with a half-life of 77.236 days by emitting several gamma rays, among others the two strongest 846.77 keV (99.94%) and 1238.29 keV (66.46%).

The experimental ^{56}Co spectrum as a result of the proton-irradiated ^{56}Fe target, measured using the NaI(Tl) detector, is given in Figure 3, which shows the two main gamma rays emitted by the ^{56}Co radionuclide at 847 keV and 1238 keV along with an annihilation peak at 511 keV being ^{56}Co , a positron emitter. The high count rate and the change in count rate were expected to be sufficient for the degradation measurement. In terms of radiation protection, with a total radioactivity of just 425 kBq (11.5 μCi) measured in the target, there was no immediate concern over the safety of the radiation workers. Note that the whole

experiment was performed in the cyclotron facility laboratories at PTRR – BATAN, which have been licensed by the Nuclear Energy Control Board of Indonesia (BAPETEN) and also accredited by the National Standardization Agency (BSN) as well as the National Committee for Accreditation of Research and Development Institutions (KNAPP).

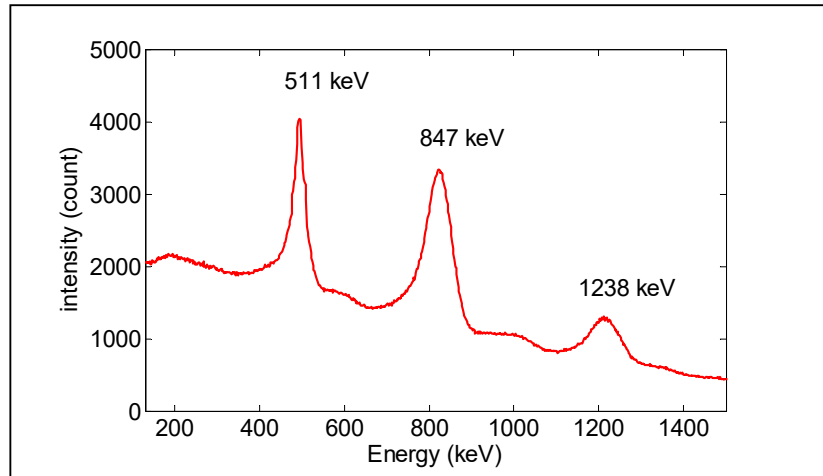


Figure 3 Measured energy spectrum of ^{56}Co in Fe target at a measuring time of 5 minutes.

While natural iron contains 91.75% of ^{56}Fe , 5.85% of ^{54}Fe , 2.12% of ^{57}Fe and 0.28% of ^{58}Fe , during the 10-MeV proton bombardment the most significant nuclear reaction to occur was $^{56}\text{Fe}(p,n)^{56}\text{Co}$ reaction, whereas according to the TALYS calculated data, other reactions such as $(p, 2n)$ occur at a proton threshold energy of 15.7 MeV, while $(p, 2p)$ only happens at a proton threshold energy of 10.3 MeV. Moreover, with proton energy at 10 MeV there was no significant change in the production of ^{55}Fe and other radionuclides due to the relatively low energy proton irradiation as well as the low excitation functions of the other nuclear reactions.

3.3 Experimental Calibration Curve

The experimental calibration curve derived from the radioactivity measurement of each iron foil is plotted in Figure 4(A), which indicates that the ^{56}Co radioactivity remains significantly detectable when the foil thickness is $195 \pm 64 \mu\text{m}$. The radioactive layer obtained from the experimental result (between 131 and 259 μm) was in good agreement with the expected theoretical calculation of 160.4 μm thickness, as discussed in Section 3.1. The gamma ray intensity dropped to the same rate as the background (equal to 3% or less of its

maximum count) when the Fe thickness was over 200 μm . This typical calibration curve, which plots the depth of penetration or the foil thickness against the relative radioactivity, was used for the remaining activity method with the TLA technique. For comparison, the calibration curve for the concentration method is presented in Figure 4(B), in which the relative activity increases exponentially with increasing thickness or depth of penetration.

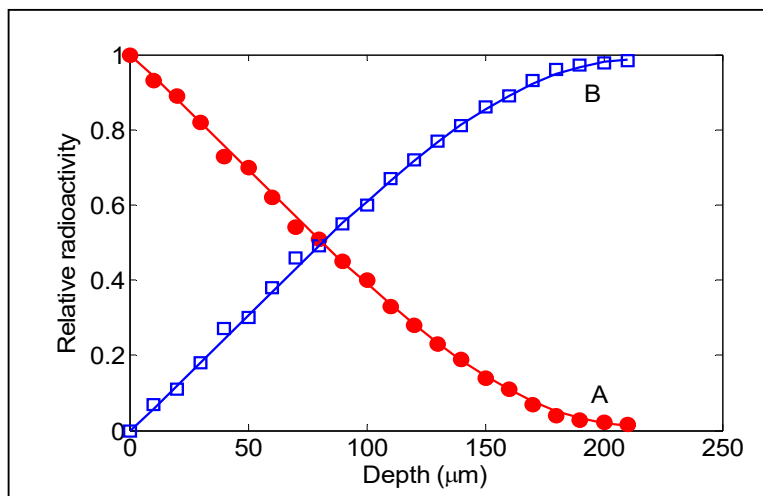


Figure 4 Experimental calibration curves used for (A) remaining activity method and (B) concentration method.

3.4 Measured Flow-Induced Erosion Rates of Iron

TLA analysis is only applicable when the flow-induced corrosion is followed by surface loss of the coupon since this corresponds to the radioactivity loss. By measuring the radioactivity ratio at a certain time while exposing the specimens to the moving fluid, one can precisely determine the degradation rates of the coupon. The measured degradation rates are plotted in Figure 5 for the measurements using the remaining activity method (filled circles) and for those using the concentration method (unfilled squares). It is clear from the figure that there was no significant difference between the results of both methods. Early on during the FIC measurement, a surface loss rate of $10.28 \pm 3.6 \mu\text{m/hr}$ was recorded, whereas the surface loss became much slower and leveled off to a steady rate of $0.91 \pm 0.30 \mu\text{m/hr}$ when the measuring time was over 15 hours.

The high erosion rate observed at the early stages of the measurement was most likely due to the pressure increase in the flowing seawater as the fluid was pumped into the system. Nevertheless, it should be noted that the steady rate of

$0.91 \pm 0.30 \mu\text{m/hr}$ recorded at a measuring time of greater than 15 hours is understood to be the true rate for this experimental condition.

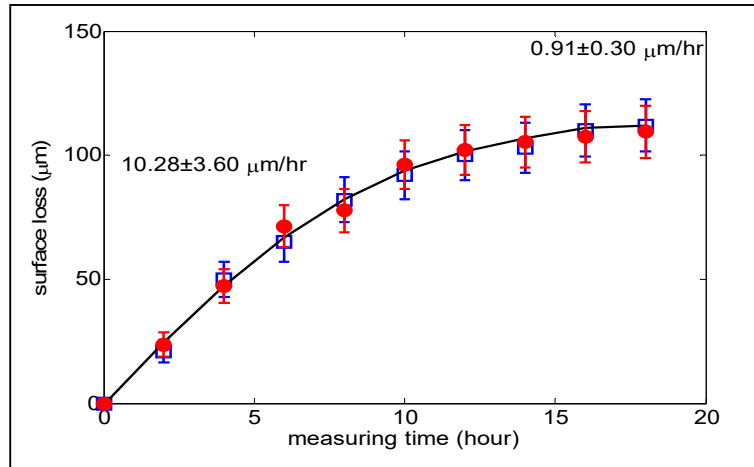


Figure 5 Experimental surface loss of the iron target as a function of time measured using the remaining activity method (filled circles) and the concentration method (unfilled squares).

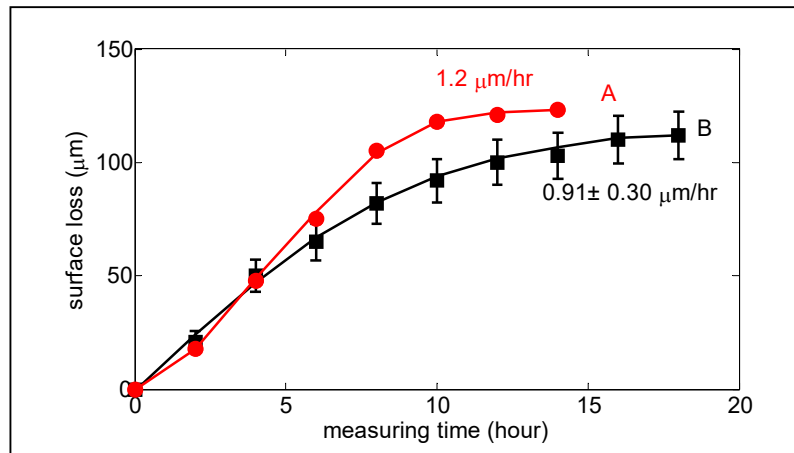


Figure 6 Flow-induced erosion rates of iron in (A) solution of 0.001 M HCl [11], and (B) seawater.

In fact, the degradation rate of the iron coupon in seawater (Figure 6(B)) was lower than that of iron in 0.001 M HCl solution (Figure 6(A)), which has been reported in [15]. The added acid solution increased the surface loss of the iron

specimen, though in the early stages (measuring time between 0 and 5 hours) the degradation rate was comparable.

In this experiment, the most notable source of uncertainties that may contribute to measurement errors is the statistical variation of the count reading, including the energy of incident radiation, which is often unknown due to scatter and absorption, as well as detector dead time.

4 Conclusion

The thin layer activation (TLA) technique was proven to be applicable for measuring extremely low surface loss of iron specimens in seawater. Using the laboratory-scaled erosion-corrosion testing facility at the BATAN's Center for Radioisotope and Radiopharmaceutical Technology (PTRR) in Serpong, we were able to simulate flow-induced erosion of iron surfaces. ^{56}Co radionuclide layers on iron surfaces could be produced via a $^{56}\text{Fe}(p,n)^{56}\text{Co}$ nuclear reaction using a 10-MeV proton beam. By exposing the ^{56}Co labeled iron coupons to circulating seawater simulated in BATAN's flow-induced erosion test facility, the surface loss of the specimens could be measured. The experimental results indicated that the TLA technique was able to measure a very low flow-induced erosion rate of $0.91 \pm 0.30 \mu\text{m/hr}$. There was no significant difference in the measured surface loss rates between the remaining activity method and the concentration method. The iron surface loss in seawater was found to be lower than that of the same specimen in HCl solution.

Acknowledgements

This research was fully funded by the Indonesian National Nuclear Energy Agency (BATAN). The authors would like to gratefully to all Cyclotron Division staff for their invaluable technical assistance.

References

- [1] Fehsenfeld, C., Fehsenfeld, P., Kleinrahm, A., Berlet, P. & Erhard, Ph., *Online Wear Measurements in Advanced Lubricated Systems*, in Friction, Wear and Wear Protection, Fischer, A. & Bobzin, K. (eds.), Wiley-VCH Verlag GmbH & Co. KGaA, Weinheim, Germany, pp. 431-438, 2011.
- [2] Corniani, E., Jech, M., Wopelka T., Ditroi, F., Franek, F. & Pauschitz, A., *High-Resolution Wear Analysis of a Ball-on-Disc Contact Using Low-Activity Radioactive Isotopes*, Journal of Mechanical Engineering Science, **226**(2), pp. 319-326, 2012.
- [3] Corniani, E., Jech, M., Ditroi, F., Wopelka, T. & Franek, F., *TLA and Wear Quantification of an Aluminium-Silicon-Copper Alloy for the Car Industry*, Wear, **267**(5), pp. 828-832, 2009.

- [4] Conlon, T.W., *Thin Layer Activation by Accelerated Ions: Application to Measurement of Industrial Wear*, *Wear*, **29**(1), pp. 69-80, 1974.
- [5] Deterding, J.H. & Calow, J.R.B., *Piston Ring Wear*, *Automobile Engineer*, **48**, pp. 378-381, 1958.
- [6] Ditroi, F., Takacs, S., Tarkanyi, F., Reichel, M., Scherge, M. & Gerve, A., *Thin Layer Activation of Large Areas for Wear Study*, *Wear*, **26**, pp. 1397-1400, 2006.
- [7] Sauvage, T., Vincent, L., & Blondiaux, G., *Thin Layer Activation (TLA) and Ultra Thin Layer Activation (UTLA): Two Complementary Techniques for Wear and Corrosion Studies in Various Fields*, in Proc. the International Conference on Applications of High Precision Atomic and Nuclear Methods, **36**(48), pp. 125-135, 2005.
- [8] IAEA, *The Thin Layer Activation Method and its Applications in Industry*, IAEA TECDOC 324, Vienna, 1997, http://www-pub.iaea.org/MTCD/publications/PDF/te_0924_scr.pdf (16 October 2014).
- [9] Singh, D.P., Sharma, V.R., Yadav, A., Singh, P.P., Unnati, Sharma, M.K., Bhardwaj, H.D., Singh, B.P. & Prasad, R., *Surface Wear Studies in Some Materials Using α -induced Reactions*, *Journal of Nuclear Physics, Material Sciences, Radiation and Applications*, **1**(1), pp. 13-24, 2013.
- [10] Craciun, L., Dudu, D., Hermann, S.C.H. & Ivanov, E.A., *Status and Perspectives at the IFIN-HH Cyclotron for Materials Analysis and Characterization*, *Romanian Reports in Physics*, **61**(3), pp. 501-512, 2009.
- [11] Chowdhury, D.P., Datta, J. & Reddy, A.V.R., *Applications of Thin Layer Activation Technique for the Measurement of Surface Loss of Materials: An Indian Perspective*, *Radiochim. Acta*, **100**, pp. 139-145, 2012.
- [12] Subramanian, H., Madasamy, P., Kumawat, H., Thomas, R.G., Krishnamohan, T.V., Velmurugan, S. & Narasimhan, S.V., *Thin Layer Activation for Probing Flow Accelerated Corrosion of Carbon Steel*, *Corrosion Science*, **54**, pp. 45-51, 2012.
- [13] Soares, C.G., Garbatov, Y. & Zayed, A., *Effect of Environmental Factors on Steel Plate Corrosion under Marine Immersion Conditions*, *Corrosion Engineering, Science and Technology*, **46**(4), pp. 524-541, 2011.
- [14] Kambali, I., Suryanto, H. & Parwanto, *Radioactive by-Products of a Self-Shielded Cyclotron and the Liquid Target System for F-18 Routine Production*, *Australas. Phys Eng Sci Med*, **39**(2), pp. 403-412, 2016.
- [15] Kambali, I. & Suryanto, H., *Interaction of High Energy Proton in Matter and Its Application for Corrosion, Erosion and Wear Studies of Materials*, *Journal of Radioisotope and Radiopharmaceutical*, **7**(2), pp. 16-21, 2004.
- [16] Ziegler, J.F., Ziegler, M.D. & Biersack, J.P., *SRIM—The Stopping and Range of Ions in Matter*, *Nucl. Inst. Meth. Phys. Res. B*, **268**, pp. 1818-1823, 2010.

- [17] Paul, H., *Comparing Experimental Stopping Power Data for Positive Ions with Stopping Tables, Using Statistical Analysis*, Nucl. Inst. Meth. Phys. Res. B, 273, pp. 15-17, 2012.
- [18] Zhao, W., Lu, H. & Yu, W., *Measurement of Cross Sections by Bombarding Fe with Protons up to 19 MeV*, Chinese Journal of Nuclear Physics, **15**(4), pp. 337-340, 1993.
- [19] Levkovskij, V.N., *Activation Cross Section Nuclides of Average Masses ($A=40-100$) by Protons and Alpha-Particles with Average Energies ($E=10-50$ MeV)*, Act. Cs., Moscow 1991.